Status of the QUAX experiment

Lab @INFN-**LNL**

C. Braggio (this presentation), G. Carugno, N. Crescini, R. Di Vora, A. Ortolan, G. Ruoso, A. Lombardi, R. Pengo, L. Taffarello

100 μW at 100 mK

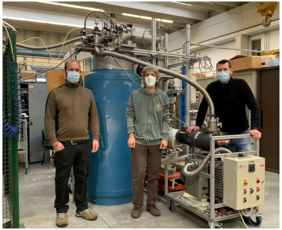

1 mW at 100 mK

Lab @INFN-**LNF**

C. Gatti, D. Alesini, D. Babusci, A. D'Elia, D. Di Gioacchino, C.Ligi, G. Maccarrone, A. Rettaroli, S. Tocci

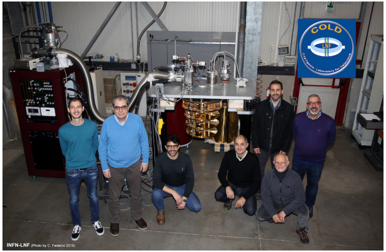

@INFN-**Salerno**
U. Gambardella, G. Iannone, CD. D'Agostino
@INFN-**Trento**
P. Falferi, R. Mezzena

QUAX COLLABORATION ROADMAP (2021-2025)

INFN
Istituto Nazionale di Fisica Nucleare

→ DM axion search (axion-photon coupling) by scanning (8.5 – 11) GHz frequency range at KSVZ sensitivity

→ **LNL** and **LNF** INFN laboratories will work in synergy, operating in **different mass ranges** and using **different low noise amplifiers and single microwave photon detectors**.

→ EU and US collaborations for the integration of:

1. **high-Q cavities** (SQMS, Superconducting Quantum Materials and Systems Center, led by Fermilab)
2. state-of-the-art **itinerant microwave photon counters** (Quantronics group, Saclay)
3. **traveling wave PA** (N. Roch group, Néel Institute in Grenoble)

SQMS SUPERCONDUCTING QUANTUM MATERIALS & SYSTEMS CENTER

cea Quantronics Group
Research Group in Quantum Electronics, CEA-Saclay, France

NÉEL institut

HALOSCOPE - resonant search for axion DM in the Galactic halo

- original proposal by P. Sikivie (1983)
- search for axions as cold dark matter constituent: SHM from Λ_{CDM}, local DM density ρ
  - $\rightarrow$ signal is a **line** with 10^{-6} relative width in the energy($\rightarrow$ frequency) spectrum
  - $\rightarrow$ + sharp (10^{-11}) components due to non-thermalized
- an **axion** may interact with a **strong** $\vec{B}$ **field** to produce a **photon** of a specific frequency ($\rightarrow m_a$)

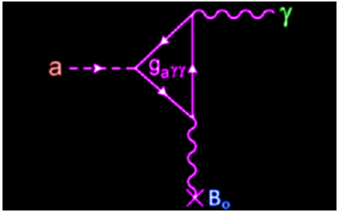

QUAX collaboration roadmap (2021-2025)

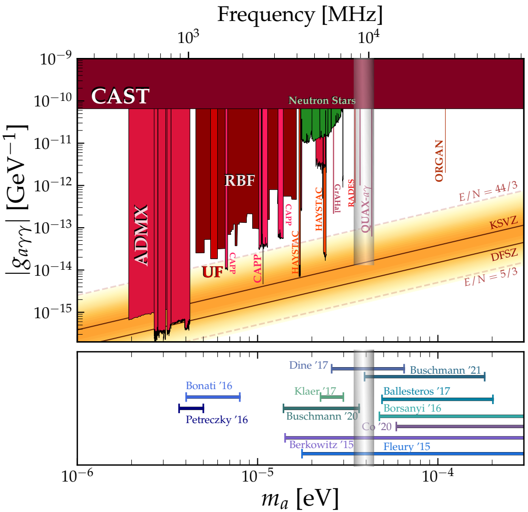

	LNF	LNL
Magnetic field	9 T	14 T
Magnet length	40 cm	50 cm
Magnet inner diameter	9 cm	12 cm
Frequency range	8.5 - 10 GHz	9.5 - 11 GHz
Cavity type	Hybrid SC	Dielectric
Scanning type	Inserted rod	Mobile cylinder
Number of cavities	7	1
Cavity length	0.3 m	0.4 m
Cavity diameter	25.5 mm	58 mm
Cavity mode	TM010	pseudoTM030
Single volume	$1.5 \cdot 10^{-4}$ m^3	$1.5 \cdot 10^{-4}$ m^3
Total volume	7⊗0.15 liters	0.15 liters
Q_0	300 000	1 000 000
Single scan bandwidth	630 kHz	30 kHz
Axion power	$7 \otimes 1.2 \cdot 10^{-23}$ W	$0.99 \cdot 10^{-22}$ W
Preamplifier	TWJPA/INRIM	DJJAA/Grenoble
Operating temperature	30 mK	30 mK

OUTLINE

1. data analysis results of July 2021 run with **high-Q dielectric resonator**
   8 T-field, HEMT readout, 1 MHz-tuning at 10.353 GHz ($m_a = 42.8\,\mu$eV)

2. **TWPA**-based amplification chain characterization
   generic input test cavity

3. July 2022 run with the dielectric resonator ($\nu_{030} = 10.353$ GHz)
   8 T-field, TWPA readout at 10 GHz

4. **Single Microwave Photon Detectors for "itinerant" photons**:
   - preparation of a transmon based-SMPD haloscope readout experiment
     3 T-field, 7 GHz NbTi cavity, 10 MHz-tuning
   - preliminary results obtained a underdamped Josephson junction (L. Kuzmin) coupled to a generic input test cavity

dielectric cavity

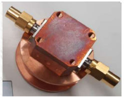

TWPA amplifier

NbTi cavity

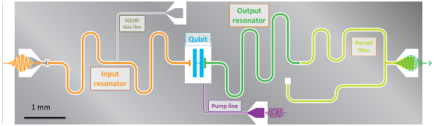

trasmon-based SMPD

DIELECTRIC CAVITY

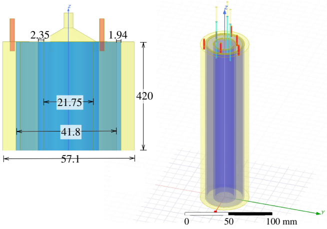

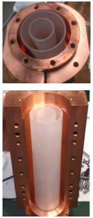

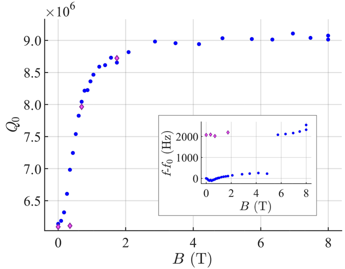

- copper cavity with dielectric shells / "dielectric boosted" resonator concept
  Phys. Rev. Appl. 14, 044051 (2020)
  J. Phys. G47 035203 (2020)
- the shells allow for shaping the cavity fields to suppress ohmic losses at the copper boundaries
  - higher order modes (e.g. TM_{030}) are exploited $C_{030} = 0.03$ (2-shell), upcoming version with 1-shell has $C_{030} = 0.47$ ($df/dt \propto C^2 Q$)
- ⊗ paramagnetic impurities in sapphire have indeed several zero point field transitions around the TM_{030} frequency
- ⊗ their energy change at the rate $df/dB \sim 28\,\mathrm{GHz/T}$ → at high B-fields they are completely swept away from ν_c

Phys. Rev. Appl. 17, 054013 (2022)

Measurement scheme

- two weeks data taking (June 2021)
- cavity excess-power searched in a small frequency band about 10.353 GHz ($\sim 42.8\mu$ eV axion mass)
- three different configurations:
  1. $\beta \simeq 1$, i.e. $Q_L > Q_a$
  2. $\beta \simeq 6$, i.e. $Q_L \simeq Q_a$
  3. $\beta \gtrsim 14$, i.e. $Q_L < Q_a$
- $T_{\text{sys}} = 17.3 \pm 1\,\text{K}$ $\qquad T_{\text{sys}} = \dfrac{P_0}{kBg_3}$

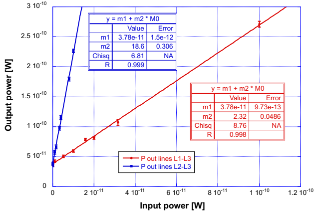

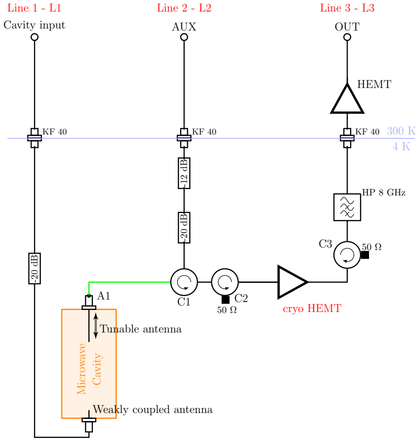

- a posteriori measured $T_A = 10 - 12\,\text{K}$ instead of the nominal noise temperature of 4.5 K, cryo HEMT sent for repair

Results

1. $\beta \simeq 1$, i.e. $Q_L > Q_a$
2. $\beta \simeq 6$, i.e. $Q_L \simeq Q_a$
3. $\beta \gtrsim 14$, i.e. $Q_L < Q_a$

issues regarding possible systematics for cases 1) and 2) $\longrightarrow$ we focused on $Q_L < Q_a$, with $Q_L \sim 3 \times 10^5$

- Haystac data analysis procedure
- even with a **very bad receiver**, to operate the high-Q cavity allowed for probing realistic QCD axion models, only marginally outside the benchmark QCD axion band
- axion mass not accessible to other running experiments

Results submitted for publication last week

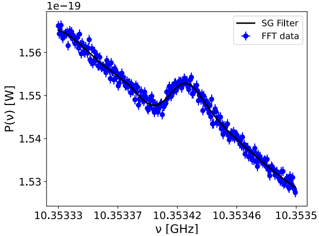

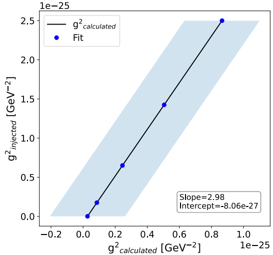

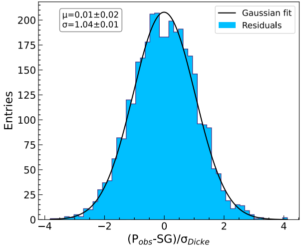

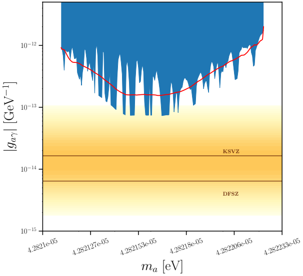

OUTLINE

1. data analysis results of July 2021 run with high-Q dielectric resonator
   8 T-field, HEMT readout, 1 MHz-tuning at 10.353 GHz ($m_a = 42.8\,\mu$eV)

2. TWPA-based amplification chain characterization
   generic input test cavity

3. July 2022 run with the dielectric resonator ($\nu_{030} = 10.353\,$GHz)
   8 T-field, TWPA readout at 10 GHz

4. preparation of a single microwave photon counter (SMPD) experiment
   3 T-field, 7 GHz NbTi cavity, 10 MHz-tuning

dielectric cavity

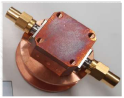

TWPA amplifier

NbTi cavity

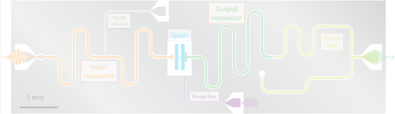

trasmon-based SMPD

Traveling Wave Parametric Amplifiers

In haloscope search amplifiers with **quantum-limited noise performance** and $\sim$ **GHz amplification bandwidth** are needed.
Standard resonant parametric amplification puts a constraint on the amplification bandwidth. This limitation can be overcome with TWPAs.

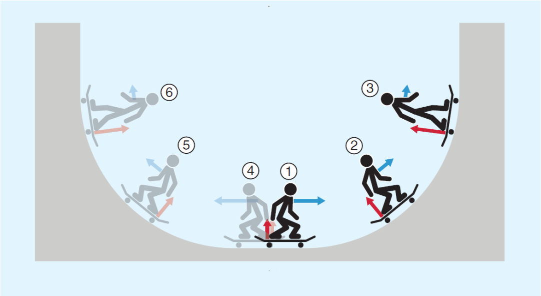

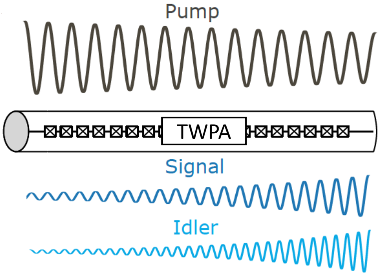

Josephson metamaterial and Reversed-Kerr phase matching

- **tunable**, **nonlinear** unit element is the "snail"
- phase matching between pump, signal and idler fields is accomplished via **reversed kerr** phase matching

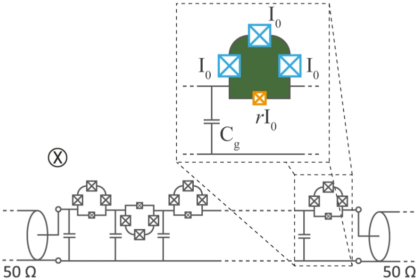

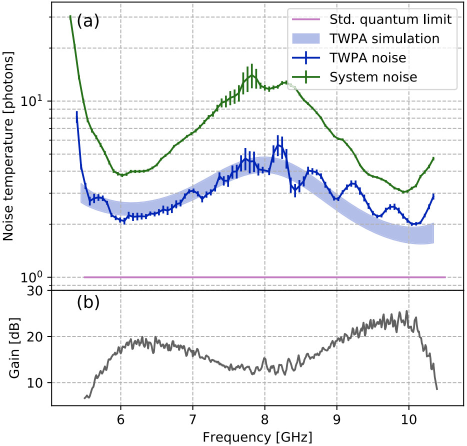

A. Renadive *et al*, Nat. Commun. 13, 1737 (2022)
M. Esposito *et al* Appl. Phys. Lett. 119, 120501 (2021)
M. Esposito *et al* Phys. Rev. Lett 128, 153603 (2022) ⟸ **broadband squeezing!**

Measuring TWPA performance in a haloscope setup

He^3-He^4 “wet” dilution refrigerator (refurbished) $\rightarrow$ recovery system + compressor at LNL




1 mW cooling power at 120 mK
$T_{mc} = 55$ mK
8 T-magnet, charging at 0.07 mA/s ; a 14 T magnet is coming in 2023

Measuring TWPA performance in a haloscope setup

Novel, reliable calibration scheme to measure T_n **exactly at the cavity output** and **without the need for switches nor heated load**.

Measuring receiver gain (A1-L4) and noise power at the cavity output and same parameters for the TWPA

- inject calibrated signals down L1 and L3
- record spectra at L4 and L1 outputs
- perform straight-line fits to obtain line gains

$$P_{out}^{xy} = P_n^{xy} + G^{xy} \cdot P_{in} \qquad (xy) = \{14, 34, 31\}$$

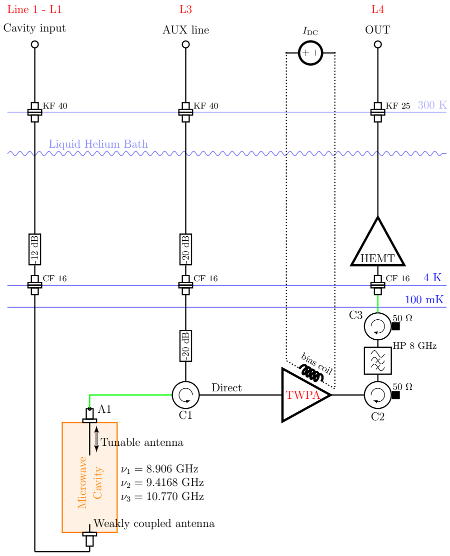

Measuring TWPA performance in a haloscope setup

- overall detection **gain**, from G_{xy}s

$$g_4 = \sqrt{\frac{G_{14}G_{34}}{G_{31}}}$$

- system **equivalent noise temperature**, referring noise power at L4 output to the input:

$$P_n^{xy} = g_4 k T_{sys} B + N_{SA} \qquad (xy) = \{14, 34\}$$

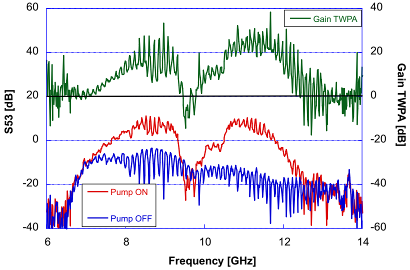

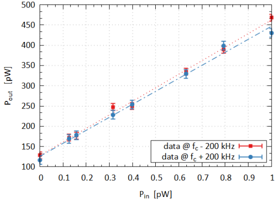

➢ Fit L3 → L4

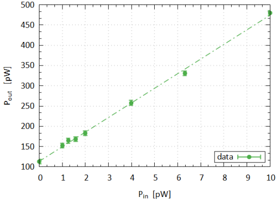

➢ Fit L1 → L4

- reduced **gain ripples** compared to state-of-the-art TWPAs
- in-situ **tunability of amplification bandwidth** over an unprecedented wide range

arXiv:2205.02053

Measuring TWPA performance in a haloscope setup

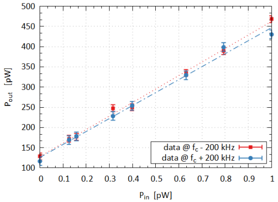

➤ Fit L3 → L4

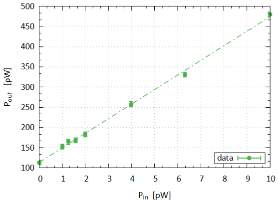

➤ Fit L1 → L4

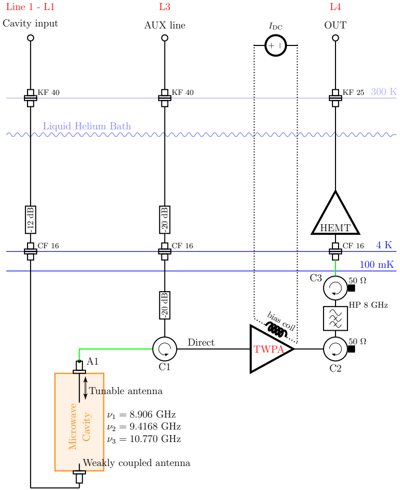

- figures of merit for the **complete detection chain**

$$g_4(\text{dB}) = (76.4 \pm 0.1) \qquad T_{sys} = (2.01 \pm 0.06)\,\text{K}$$

- figures of merit for the **TWPA**

$$G_{\text{TWPA}}(\text{dB}) = 24 \qquad T_{\text{TWPA}} \approx 1.8\,\text{K}$$

arXiv:2205.02053

SMPDs: motivation

- $\odot$ QUAX$_{a-e}$, the ferrimagnetic haloscope
  Phys. Rev. Lett. 124, 171801 (2020)

- $\odot$ QUAX$_{a-\gamma}$ at 10 GHz

– "Game changer at high frequency and low temperatures" : a photon counter measures in the **energy eigenbasis** - beyond SQL

– $\mathrm{SNR}_{\mathrm{exc}} = \frac{P_{a\to\gamma}}{kT_{\mathrm{sys}}}\sqrt{\frac{t_m}{\Delta\nu_a}}$ $\quad$ $\mathrm{SNR}_{\mathrm{SMPD}} = \frac{P_{a\to\gamma}}{h\nu}\sqrt{\frac{t_m}{\Gamma_{dc}}}$

$$\frac{\mathrm{SNR}_{\mathrm{SMPD}}}{\mathrm{SNR}_{\mathrm{exc}}} > 1 \iff \frac{\Gamma_{dc}}{\eta} < \frac{\nu_a}{10^6}$$

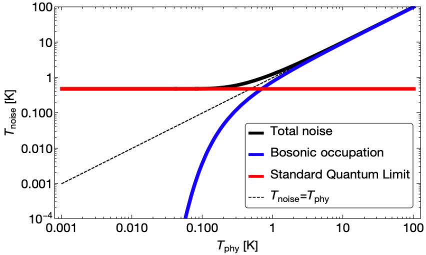

plot example at 10 GHz given on Tue by SungWoo YOUN

quantum advantage can be shown even with relatively high dark count rates Γ_{dc}

ELECTRON COUPLING – QUAX *the FMR haloscope*

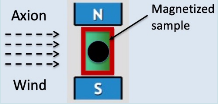

the axion DM cloud acts as an **effective RF magnetic field** on the electron spin exciting **magnetic transitions** in a magnetized sample (YIG) → **RF photons**

$$P_{\text{out}} = \frac{P_{\text{in}}}{2} = \mathbf{3.8 \times 10^{-26}} \left(\frac{m_a}{200\,\mu\text{eV}}\right)^3 \left(\frac{V_s}{100\text{ cm}^3}\right) \left(\frac{n_S}{2 \cdot 10^{28}/\text{m}^3}\right) \left(\frac{\tau_{\min}}{2\,\mu\text{s}}\right) \text{W}$$

ESR (Electron Spin Resonance)
the RF field is actually the axion effective field
—>> axion mass tuning with B field!
1.7 T —> 48 GHz

YIG (Yttrium Iron Garnet)

$\tau_{\min} = \min(\tau_a, \tau_c, \tau_2)$

under the condition of **strong coupling**

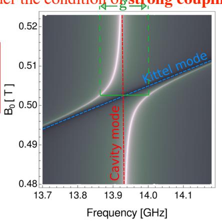

$$R_a = \frac{P_{\text{out}}}{\hbar\omega_a} = \mathbf{1.2 \times 10^{-3}}\text{ Hz}$$

corresponding signal photon rate

SMPDs for itinerant photons

A Single Photon Microwave Counter (SMPD) architecture is significantly different whether it is meant for **cavity photons** or **itinerant (traveling) photons**.
We are interested in the itinerant version due to the intense magnetic fields involved in axion search.

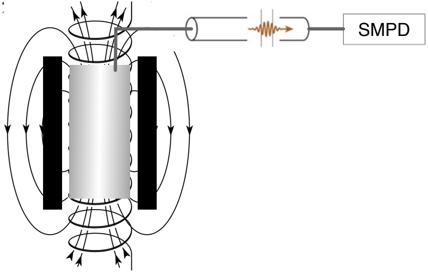

- detection of individual microwave photons is a challenging task because of their **low energy** $\sim 10^{-5}$ eV
- a solution: use "**artificial atoms**" introduced in circuit QED, their transition frequencies lie in the ∼GHz range
- or: rely on a single **current-biased Josephson junction** (L. Kuzmin)

ARTIFICIAL ATOMS: the TRANSMON QUBIT

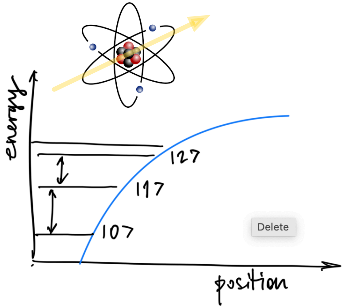

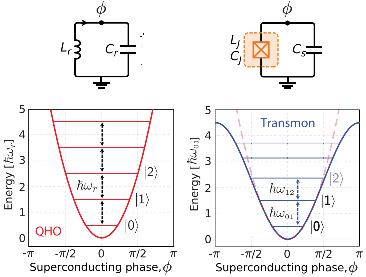

$E_{01} = E_1 - E_0 = \hbar\omega_{01} \neq E_{02} = E_2 - E_1 = \hbar\omega_{21}$
$\rightarrow$ good **two-level atom** approximation

control internal state by shining laser tuned at the transition frequency:
$H = -\vec{d} \cdot \vec{E}(t)$, with $E(t) = E_0 \cos\omega_{01} t$

toolkit: capacitor, inductor, wire (all SC)
$\omega_{01} = 1/\sqrt{LC} \sim 10\,\mathrm{GHz} \sim 0.5\,\mathrm{K}$
$\rightarrow$ simple LC circuit is not a good **two-level atom** approximation

$I_J = I_c \sin\phi \qquad V = \frac{\phi_0}{2\pi}\frac{\partial\phi}{\partial t}$

$V = \frac{\phi_0}{2\pi}\frac{1}{I_c\cos\phi}\frac{\partial I_J}{\partial t} = L_J\frac{\partial I_J}{\partial t}$

$L_J = \frac{\phi_0}{2\pi}\frac{1}{I_c\cos\phi}$ NL Josephson inductance

transmon-based SMPD

In the Quantronics group (CEA, Saclay) a transmon-based counter has been developed and used to make spin fluorescence measurements, paving the way to **single spin flip detection** with SMPDs.

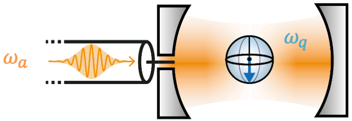

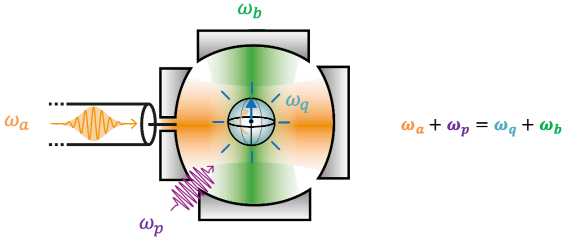

R. Lescanne *et al*, Phys. Rev. X 10, 021038 (2020)
E. Albertinale *et al*, Nature 600, 434 (2021)

Quantronics Group
Research Group in Quantum Electronics, CEA-Saclay, France

transmon-based SMPD

In the Quantronics group (CEA, Saclay) a transmon-based counter has been developed and used to make spin fluorescence measurements, paving the way to **single spin flip detection** with SMPDs.

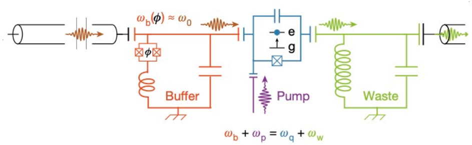

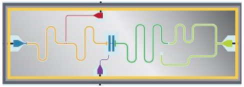

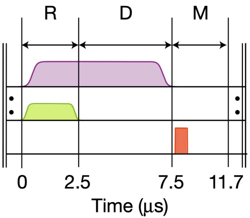

R. Lescanne *et al*, Phys. Rev. X 10, 021038 (2020)
E. Albertinale , Nature 600, 434 (2021)

Quantronics Group
Research Group in Quantum Electronics, CEA-Saclay, France

- a three-step process repeated several times
- qubit reset (R) performed by turning on the pump pulse + a weak resonant coherent pulse to the waste port
- detection (D) step with the pump pulse on
- measurement (M) step probes the dispersive shift of the buffer resonator to infer the qubit state

QUANTUM SENSING

"Quantum sensing" describes the use of a quantum system, quantum properties or quantum phenomena to perform a measurement of a physical quantity
Rev. Mod. Phys. 89, 035002 (2017)

1. Use of a **quantum object** to measure a physical quantity (classical or quantum). The quantum object is characterized by quantized energy levels, i.e. electronic, magnetic or vibrational states of superconducting or spin qubits, neutral atoms, or trapped ions.
2. Use of **quantum coherence** (i.e., wave-like spatial or temporal superposition states) to measure a physical quantity
3. Use of **quantum entanglement** to improve the sensitivity or precision of a measurement, beyond what is possible classically.

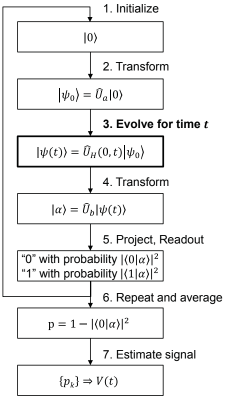

BASIC PROTOCOL

quantum sensing experiments typically follow a generic sequence of processes known as:

1. sensor initialization into a known basis state
2. interaction with the signal
3. sensor readout
4. signal estimation

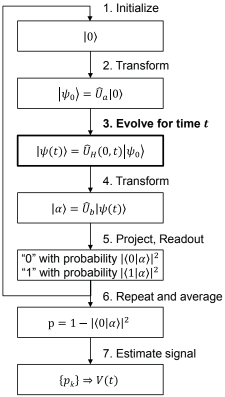

Pilot SMPD-haloscope experiment

- copper cavity **sputtered with NbTi**
  magnetron sputtering in INFN-LNL
- right cylinder resonator, TM_{010} mode
  $\nu_c \sim 7.3\,\text{GHz}$ to match the new generation SMPD bandwidth (7.280 - 7.380) GHz
- **system of sapphire triplets** to tune the cavity frequency
  ~ 10 MHz tuning without impacting Q
- **Attocube nanopositioner** to change the sapphire rods position

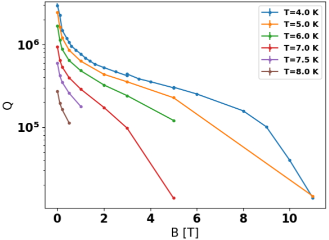

PILOT SMPD-HALOSCOPE EXPERIMENT

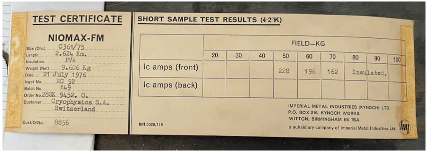
TEST CERTIFICATE

NIOMAX-FM

Size (Dia.) C361/75
Length 2.624 Km.
Insulation PVA
Weight (Net) 9.606 Kg
Date 21 July 1976
Ingot No. RC 52
Batch No. 149
Order No. 280K 9452. 0.
Customer Cryophysics S.A. Switzerland
Cust/O/No. 8856

SHORT SAMPLE TEST RESULTS (4·2°K)

	FIELD—KG								
	20	30	40	50	60	70	80	90	100
Ic amps (front)				228	196	162	Insulated.		
Ic amps (back)									

IMI 5020/118

IMPERIAL METAL INDUSTRIES (KYNOCH) LTD.
P.O. BOX 216, KYNOCH WORKS
WITTON, BIRMINGHAM B6 7BA
a subsidiary company of Imperial Metal Industries Ltd.

- copper cavity **sputtered with NbTi**
  magnetron sputtering in INFN-LNL
- right cylinder resonator, TM_{010} mode
  $\nu_c \sim 7.3$ GHz to match the new generation SMPD bandwidth (7.280 - 7.380) GHz
- **system of sapphire triplets** to tune the cavity frequency
  $\sim$ 10 MHz tuning without impacting Q
- **Attocube nanopositioner** to change the sapphire rods position
- developed and tested a **3 T magnet**
  (U. Gambardella, INFN Salerno)

More cooling power coming soon. . .

Leiden Cryogenics
commissioning in October 2022

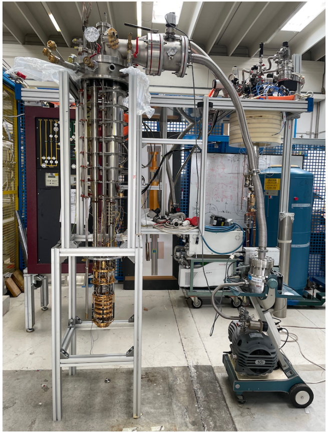

“wet” delfridge from PTB
(ongoing refurbishing)

Not that **practical** to use …but that's it!

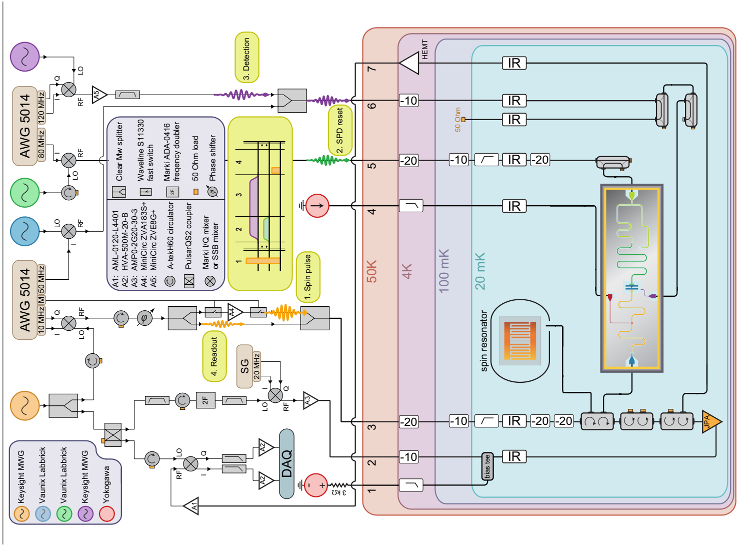

Current-biased Josephson Junction

"washboard potential"

working principle:

- voltage switching of an underdamped JJ
- phase diffusion regime

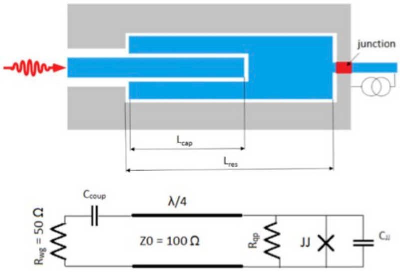

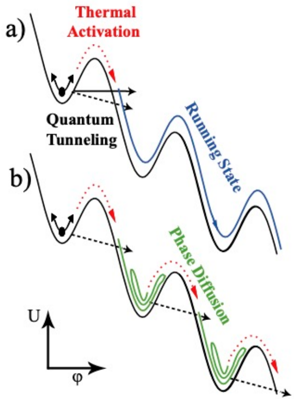

L.S. Kuzmin *et al* IEEE Trans Appl Supercond 28, 2400505 (2018);
A. L. Pankratov *et al* npj Quantum Information 8:61 (2022)

QUAX Haloscope at LNF

Probe KSVZ axions in 1 GHz band at 9 GHz
- Multi cavity for fast scanning rate
- Wide band TWJPA quantum amplifier
- Superconducting cavities

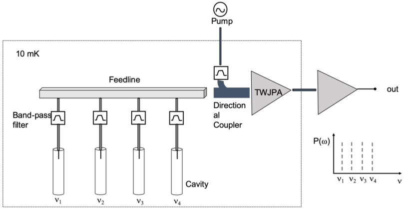

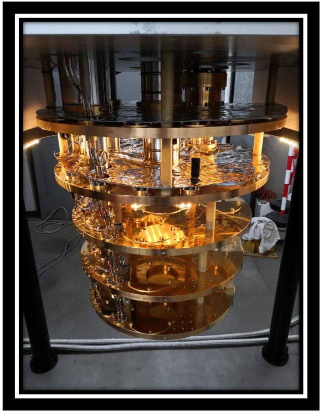

Leiden CF-CS-110-1000 dilution refrigerator with 8 mK base temperature

9 T magnet from AMI

First run with single 8.5 GHz OFHC Cu cavity

- Cu cavity
- HEMT amplifier
- No tuning system yet
- Auxiliary lines for gain calibration

- $V = 0.141\ l$
- $f = 8.5$ GHz
- $m_a = 35\ \mu eV$
- $Q_0 = 100{,}000$
- $\beta=1$
- $C_{010} = 0.67$
- $B_0 = 2.5$ T ($B_{av}=0.865\ B_0$)
- $\Delta t = 7532\ s$
- $T_{cav} = 150$ mK
- $T_{noise} \sim 8$K

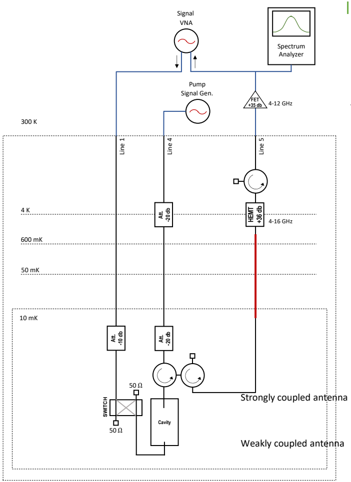

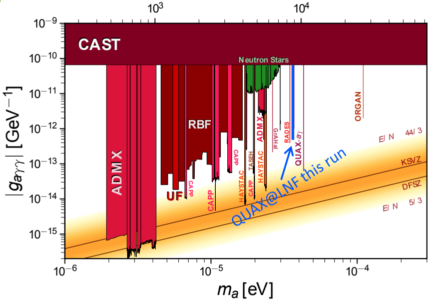

With single Cu cavity

Target (in GeV^{-1})	$g^{KSVZ} = 1.35 \times 10^{-14}$
$T_n = 8$ K, $B_0 = 2.5$ T	$g_{90\%} = 3.3 \times 10^{-13}$
$T_n = 4$ K, $B_0 = 9$ T	$g_{90\%} = 6.5 \times 10^{-14}$
$T_n = 0.5$ K, $B_0 = 9$ T	$g_{90\%} = 2 \times 10^{-14}$